Clinical Neurophysiology 130 (2019) 767–780

Contents lists available at ScienceDirect

Clinical Neurophysiology

journal homepage: www.elsevier.com/locate/clinph

Does hand robotic rehabilitation improve motor function by rebalancing interhemispheric connectivity after chronic stroke? Encouraging data from a randomised-clinical-trial

Rocco Salvatore Calabrò [a,*], Maria Accorinti [a], Bruno Porcari [a], Luigi Carioti [a], Laura Ciatto [a], Luana Billeri [a], Veronica Agata Andronaco [a], Franco Galletti [b], Serena Filoni [c], Antonino Naro [a]

[a] IRCCS Centro Neurolesi Bonino Pulejo, Messina, Italy
[b] Otorhinolaryngoiatry Unit, University of Messina, Messina, Italy
[c] Fondazione Centri di Riabilitazione Padre Pio Onlus, San Giovanni Rotondo, FG, Italy

ARTICLE INFO

Article history:
Accepted 13 February 2019
Available online 15 March 2019

Keywords:
Amadeo™
Hand rehabilitation
Frontoparietal connectivity
Sensorimotor plasticity

HIGHLIGHTS

- Robotic hand training can be helpful in improving hand motor recovery.
- Amadeo™ induces large modulations of sensorimotor rhythms and connectivity.
- Robotic training yields improvement of hand motor performance by restoring hand motor control.

ABSTRACT

Objective: The objective of this study was the evaluation of the clinical and neurophysiological effects of intensive robot-assisted hand therapy compared to intensive occupational therapy in the chronic recovery phase after stroke.
Methods: 50 patients with a first-ever stroke occurred at least six months before, were enrolled and randomised into two groups. The experimental group was provided with the Amadeo™ hand training (AHT), whereas the control group underwent occupational therapist-guided conventional hand training (CHT). Both of the groups received 40 hand training sessions (robotic and conventional, respectively) of 45 min each, 5 times a week, for 8 consecutive weeks. All of the participants underwent a clinical and electrophysiological assessment (task-related coherence, TRCoh, and short-latency afferent inhibition, SAI) at baseline and after the completion of the training.
Results: The AHT group presented improvements in both of the primary outcomes (Fugl-Meyer Assessment for of Upper Extremity and the Nine-Hole Peg Test) greater than CHT (both $p < 0.001$). These results were paralleled by a larger increase in the frontoparietal TRCoh in the AHT than in the CHT group ($p < 0.001$) and a greater rebalance between the SAI of both the hemispheres ($p < 0.001$).
Conclusions: These data suggest a wider remodelling of sensorimotor plasticity and interhemispheric inhibition between sensorimotor cortices in the AHT compared to the CHT group.
Significance: These results provide neurophysiological support for the therapeutic impact of intensive robot-assisted treatment on hand function recovery in individuals with chronic stroke.

1. Introduction

The recovery of hand function is essential to improve the quality of life of stroke survivors, given that upper extremity paresis usually determines poor motor control and function with consequential and often severe limitations in daily functions (Alt Murphy et al., 2011; Broeks et al., 1999; Lai et al., 2002). Such recovery depends on a large repertoire of functional and structural processes within the central nervous system, collectively termed neuroplasticity, which occur spontaneously or are induced by movement practise (Nudo, 2013). Intensive, repetitive, and task-oriented motor practises using neurorobotic devices (which enable

* Corresponding author at: IRCCS Centro Neurolesi Bonino Pulejo; S.S. 113, Contrada Casazza, 98124 Messina, Italy.
E-mail address: salbro77@tiscali.it (R.S. Calabrò).

https://doi.org/10.1016/j.clinph.2019.02.013
1388-2457/

or facilitate repetitive movements) assist recovery and rehabilitation (Kwakkel et al., 2008a, 2008b; Krebs and Volpe, 2013; Norouzi-Gheidari et al., 2012; Sivan et al., 2011; Pollock et al., 2014). In particular, the recovery of hand motor function after stroke has benefitted from the use of exoskeleton-based robots and end-effector systems, including the end-effectors robotic device Amadeo™ (Tyromotion GmbH; Graz, Austria), especially in the acute phase and in association with physiotherapy and/or occupational therapy (Sale et al., 2012, 2014). On the contrary, few data are available regarding patients with chronic stroke (Stein et al., 2011). Furthermore, it has been suggested that robot-mediated training may potentially enhance neuroplasticity (Turner et al., 2013) by providing a haptic interaction and a consistent bulk of proprioceptive and/or other sensory inputs to motor outputs (Cooke and Bliss, 2006; Ramos-Murguialday et al., 2012). This is reflected by different frequency-dependent power changes in the electroencephalogram (EEG) within sensorimotor areas, also during hand movements (Formaggio et al., 2013; Novakovic and Sanguineti, 2011). There are also significant changes in functional connectivity (coherence) within the fronto-parietal networks (inter- and intra-hemispheric functional connectivity) (Sergi et al., 2011) related to movement preparation and execution. Significant changes have been observed in both intracortical facilitation and inhibition and sensorimotor integration mechanisms of the primary motor cortices, assayed by Transcranial Magnetic Stimulation (TMS), related to actual motor status and functional outcome prediction, following ischaemic stroke (Nardone and Tezzon, 2002; Hara, 2015; Alia et al., 2017; Seo et al., 2018).

However, the precise neurophysiological mechanisms of robot-mediated learning with respect to the potential to induce neuroplasticity remain unclear (Brewer et al., 2007; Mehrholz et al., 2012; Maciejasz et al., 2014). The comprehension of robot-induced neuroplasticity mechanisms underpinning motor improvement, investigated using TMS and EEG (even combined), may be critical to fully understand the clinical value of these combined therapeutic approaches, to objectively monitor clinical improvement, to estimate a prognosis of motor function recovery based on the residual plasticity mechanisms, and to potentially plan patient-tailored rehabilitative methods (Alia et al., 2017). Specifically, physical therapy and neuromodulation approaches to boost functional recovery through residual brain plasticity properties can be managed (Alia et al., 2017; Calabrò et al., 2016). Therefore, the understanding of the neuroplasticity reservoir in post-stroke patients (i.e. the plasticity potential to functional recovery) can be used to individually adapt rehabilitative programmes and to implement neuromodulation strategies (Alia et al., 2017; Takeuchi and Izumi, 2015).

This study reports a prospective, randomised, parallel group, assessor-blinded trial aimed at evaluating the connectivity and plasticity mechanisms through which robotic hand therapy (utilising Amadeo™) contributes to hand motor function recovery, beyond conventional hand training. We hypothesised that robotic hand therapy might provide patients with greater clinical improvements than an equally intense occupational therapy due to the strengthening of the specific brain plasticity and connectivity functions related to motor planning and execution.

2. Methods

2.1. Trial design

Fifty in-patients with chronic post-stroke, attending the Neurorobotic Rehabilitation Unit of the IRCCS Centro Neurolesi Bonino Pulejo (Messina, Italy), were enrolled in a randomized controlled trial between January and February 2018. The trial was aimed at comparing the clinical-electrophysiological aftereffects of robotic hand rehabilitation (utilising Amadeo™) versus standard conventional hand rehabilitation. The study was approved by our local Ethics Committee, and registered at Clinical Trials.gov (NCT03292276). All of the participants provided written informed consent before study participation.

2.2. Participants

Patients were rated as eligible according to the following criteria: (i) age $\geq$ 55 years; (ii) a first, single, ischemic, supra-tentorial, chronic-stage stroke at least 6 months after the event, confirmed by T1-weighted structural whole brain Magnetic Resonance Imaging, performed at the scoring of chronic upper limb function; (iii) a Muscle Research Council score $\leq$3 concerning shoulder abduction –deltoid– elbow flexion –biceps brachii– and wrist flexion –wrist flexors); (iv) a Mini–Mental State Examination score >24 (that is, the patient was able to follow verbal instructions); (v) a Modified Ashworth Scale score of the hand muscles $\leq$2; (vi) no prior history of severe bone or joint disease; and (vii) no prior history of concomitant neurodegenerative diseases or brain surgery. Table 1 summarises the clinical-demographics characteristics.

2.3. Interventions

The patients were divided randomly into two treatment groups: AHT and CHT. The AHT patients were provided with an intensive robotic training of the affected hand using Amadeo™, whereas those in the CHT group underwent intensive conventional physiotherapy of the affected hand. Moreover, both of the groups were subjected to conventional lower limb physiotherapy and bimanual activities. Consequently, all of the patients received the same amount of treatment in terms of frequency, intensity, number, and duration of training sessions.

Amadeo™ is an end-effector device that covers the hand fingers workspace (Fig. 1). The hand is held in position by the finger-moving system through elastic bands or plasters, whilst the wrist is fixed in position by a Velcro strap (Sale et al., 2012, 2014). Amadeo™ has five independent translational degree of freedoms and permits the movements of all of the fingers (singularly or contemporarily) through rotational joints placed between the fingertip and the arm supporting the thumb laterally (equipped with two rotational joints). Hence, the robot provides the patient with intensive and repetitive training of flexion-extension movements of the fingers. Moreover, such movements can be task-oriented as they are in conjunction with visual feedback. The usefulness of robots versus conventional physiotherapy consists of the possibility offered by robots to perform highly repetitive and controlled physical training, which may induce more evident and specific network perturbation (that is, oscillatory activity and functional connectivity) as well as particular types of neuroplasticity, in which a better functional gain in terms of motor function recovery could be achieved (Balasubramanian et al., 2010; Lum et al., 2012).

The patients in the AHT group underwent 40 individual conventional 3-hour physiotherapeutic training sessions, 5 days a week for 8 weeks (starting between 9:00 am and 11:00 am). The sessions were divided into 45 min of occupational therapy (daily living and reaching activities), 45 min of biomechanical training of both upper and lower limbs, 30 min of gait training, 30 min of speech therapy, and 30 min of rest period (distributed between the sessions) followed by 45 min of robot-assisted therapy of the affected limb using Amadeo™. Each hand training session consisted of random order exercises: (i) 15 min of continuous passive motion; (ii) 25 min of assisted therapy (movements were robot-assisted according to individual performance); and (iii) 5 min of rest period

Table 1
Clinical-demographics characteristics.

Group	Age (y)	Gender	Handedness	Location	dd (m)	CoM	Clinical features	MRC	MAS	MMSE
AHT	66	M	R	r FP	8	3	Slight spastic hemiparesis	3	2	29
	64	M	R	l PO	11	3	Hand paresis	2	1	25
	70	F	R	r TP	9	1	Slight hand paresis	3	1	29
	60	F	L	l PO	11	1 + 3	Severe hemiparesis	1	2	28
	64	F	R	r FP	6	none	Severe hemiparesis	1	2	26
	70	M	R	r P	10	1 + 2	Hemiparesis, dysarthria	2	1	29
	69	M	R	l F	7	2	Moderate hand paresis	3	1	30
	67	M	R	r FP	6	3	Hand plegia	0	2	27
	65	F	R	l PO	11	2	Hand paresis	2	1	28
	60	F	L	r FT	14	4	Moderate weakness	3	1	29
	62	M	R	r FP	10	1	Hand paresis	1	2	28
	70	M	R	l PO	10	4	Hand plegia, dysarthria	0	2	25
	69	F	L	r TP	6	2	Severe hemiparesis	1	2	27
	60	F	R	l PO	8	2	Severe hemiparesis	1	2	28
	62	F	R	r FP	14	none	Hand paresis	2	1	26
	61	M	R	r P	12	2	Hand plegia, dysarthria	0	2	29
	63	F	R	l F	13	1 + 2	Severe hemiparesis	1	2	30
	61	F	R	r FP	10	4	Hand paresis	2	1	28
	67	F	L	r FT	11	3	Hand weakness, Unable to walk, dysarthria			27
	63	M	R	l PO	11	none	Hand paresis	2	1	26
	66	M	R	r TP	12	none	Slight arm paresis moderate spasticity	3	1	30
	65	F	R	l PO	12	1 + 4	Moderate hand paresis	2	1	30
	66	F	R	r FP	12	none	Hand weakness, unable to walk, dysarthria	3	1	29
	70	F	R	l PO	8	2	Moderate hand paresis	2	1	27
	63	M	R	r FP	8	4	Slight hand paresis, spasticity of leg,facial weakness	3	1	29
Mean(s.d.)	65(3)	11 M,14F	4L 21R		10(2)			1.8(1)	1.4(0.5)	28(2)
CHT	69	M	R	r P	12	1	Moderate hand paresis	2	1	26
	61	M	R	l F	10	1 + 4	Slight arm paresis	3	1	30
	70	F	L	l F	8	3 + 4	Hemiparesis, dysarthria	2	1	26
	68	F	R	r P	11	2	Moderate hand paresis	2	1	27
	64	M	R	r FP	10	4	Mild arm paralysis, severe leg;	2	1	29
	70	M	L	r TP	6	5	Hand side weakness, unable to walk, dysarthria	3	1	29
	61	F	R	l TP	11	none	Severe hemiparesis	1	2	28
	60	M	R	r P	14	3	Slight hand paresis and weakness	3	1	29
	67	M	R	l F	12	2	Hemiparesis, dysarthria	2	1	30
	62	M	L	r P	9	none	Hand weakness, unable to walk,dysarthria	2	1	26
	69	F	R	l F	13	3	Hand plegia	0	2	26
	60	F	R	l F	12	2	Hemiparesis, dysarthria	1	1	28
	68	F	R	r P	9	5	Hand plegia, dysarthria	0	2	30
	60	M	L	r FP	9	2	Severe hemiparesis	1	2	25
	66	M	R	r TP	14	3	Hand plegia	0	2	26
	60	M	R	l TP	6	none	Severe hand paresis	1	2	29
	64	F	R	r P	12	3	Hand plegia	0	2	25
	65	M	R	l F	6	1 + 3	Mild spasticity arm and hand	2	1	26
	62	F	R	r P	10	1	Severe hand paresis	1	2	29
	60	F	R	l F	10	1 + 5	Moderate hand weakness	3	1	27
	61	M	L	l F	10	3 + 5	Hand paresis	2	1	26
	64	F	R	r P	10	none	Hand paresis	2	1	26
	65	F	R	r FP	9	3	Slight hand paresis, spasticity of leg, facial weakness	3	1	29
	64	M	R	r P	14	5	Hand paresis	2	1	26
	65	M	R	l F	12	none	Hemiparesis, dysarthria	2	1	29
Mean(s.d.)	64(3)	14M, 11F	5L 20R		10(2)			1.7(1)	1.3(0.5)	27(2)
(*)	0.5	0.2		0.3	0.6	0.5	0.7	0.7	0.5	0.3

Legend: age is expressed in years; dd disease duration in months; handedness R right L left; r right hemisphere, l left hemisphere, F frontal, P parietal, O occipital, T temporal; CoM comorbidity 1 blood hypertension, 2 diabetes mellitus, 3 smoker, 4 dyslipidemia, 5 alcoholic; M male, F female; s.d. standard deviation; AHT Amadeo™ hand training, CHT conventional hand training; (*) t-test between groups at entry time; MRC Muscle Research Council of deltoid, biceps brachii, and wrist flexors; MMSE Mini–Mental State Examination; MAS Modified Ashworth Scale of hand muscles.

between the two sessions. The movement execution was standardised: the fingers were first extended for 1 s and then flexed and extended continuously for 5 s at a frequency of 0.2 Hz. The entire flexion–extension cycle lasted 6 s. The device guidance force (DGF), during assisted therapy, was adapted to each patient's progress. Specifically, the machine detected the patient's finger movements and intervened to drive and/or complete them within the span of 6 s. The amount of required assistance was recorded by the device itself. During the session, an Amadeo™–trained physiotherapist supervised each patient's intervention adherence. Distinct video–acoustic cues signalled the patient when each movement cycle began and ended (in the passive condition) and when to move (in the assisted condition).

The patients in the CHT group also underwent 40 individual conventional 3-hour physiotherapy sessions, 5 days a week for an 8–week period, between 9:00 am and 11:00 am. This training had the same characteristics described for the AHT group. Each session was then followed by a 45 min conventional hand therapy session carried out by an occupational therapist, who both performed and assisted the patient in the execution of finger movements, reproducing the same experimental conditions of the AHT group (upper limb position and constrainment, movement execution, flexion–extension finger movements, movement frequency and velocity, degree of assistance, and video–acoustic cueing). The similar setup was necessary to avoid biasing effects on sensory processing due to differences in the restraint of the wrist between

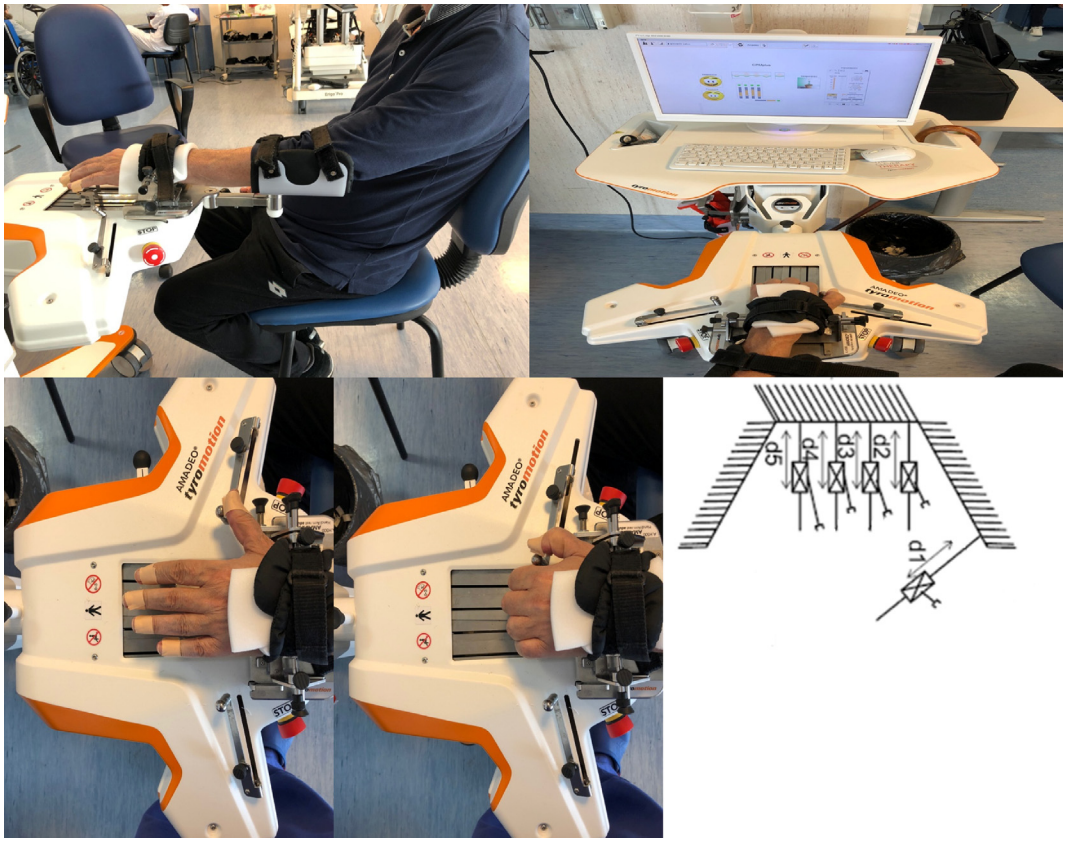

Fig. 1. Schematic image of a subject attached to the Amadeo™. The image on the right summarises the directions of the finger movements from the thumb (d1) to the little finger (d5) guided by finger sliders (small boxes).

AHT and CHT. Muscle synergies are affected by robot-dependent mechanical constraints and forces, thus affecting the sensorimotor system (Semprini et al., 2017). The patients were asked not to undertake other physiotherapy treatments during the 8-week training period.

2.4. Outcomes

The primary outcomes were the Fugl-Meyer Assessment for Upper Extremity (FMAUE) and the Nine-Hole Peg Test (9HPT). The FMAUE measures the motor function, sensation, and joint function recovery of the upper limb (that is, the movement, coordination, and reflex action at each segment of the upper limb) following stroke (Fugl-Meyer et al., 1975; Gladstone et al., 2002). Thus, useful information is gained concerning disease severity, motor recovery, and treatment efficacy. Such scale has an excellent Test-retest Reliability, Interrater–Intrarater Reliability, Criterion and construct Validity, and responsiveness (Santisteban et al., 2016; Croarkin et al., 2004).

During 9HPT, the patient has to pick up quickly a peg from a small shallow container, to put it into a hole in a wood or plastic block (containing nine empty holes). This operation is repeated nine times, using nine different pegs. Once the block has been filled with the nine pegs, the patient has to quickly remove the pegs, one at a time, replacing them into the shallow container. An experimenter measures the time required by the patient to complete the task, which is repeated twice. Therefore, 9HPT involves with many psychometric properties, including visual and sensory perception, coordination, and hand dexterity. Such scale has an excellent intra-rater reliability, convergent and predictive validity (Santisteban et al., 2016; Croarkin et al., 2004).

The effects of both conventional and robotic hand training were assessed as secondary outcomes. These consisted of the DGF (that was measured only in the patients in the AHT group; the modifications of cortical activity, using time-frequency event-related EEG (event related synchronization –ERS– and event related desynchronization –ERD) and task–related coherence (TRCoh); the magnitude of motor evoked potential (MEP) amplitude and of afferent inhibition (as assessed with short-latency afferent inhibition, SAI) from the abductor pollicis brevis muscle of the affected and unaffected upper limbs (as measures of corticospinal excitability and sensory afferent inhibition); and the magnitude of MEP and SAI from the abductor pollicis brevis muscle of the affected and unaffected upper limbs following a repetitive paired-associative stimulation (rPAS) protocol (as a measure of the sensorimotor plasticity). These measurements were performed before (PRE) and after the end of the training (POST). The patients' flow is summarised in Fig. 2.

The DGF is commonly used as a secondary outcome in nearly all trials using neurorobotic devices. It indicates the degree of assistance required by the patient to initiate, carry out, and/or complete a motor task. Consequently, the DGF magnitude usually decreases in parallel with motor function recovery (Hubbard et al., 2009; Huang et al., 2018).

Valuable information on functional brain activation related to movement, from preparation to execution, is provided through time–frequency analysis (ERS and ERD) of non–stationary signals during motor execution and imagery practises (Manganotti et al., 1998; Formaggio et al., 2013). Specifically, α and β oscillations over the premotor and primary sensorimotor areas, typically followed by a β synchronisation in the cortical areas ipsilateral to the moving limb, present a typical ERD (Pfurtscheller and Aranibar, 1977).

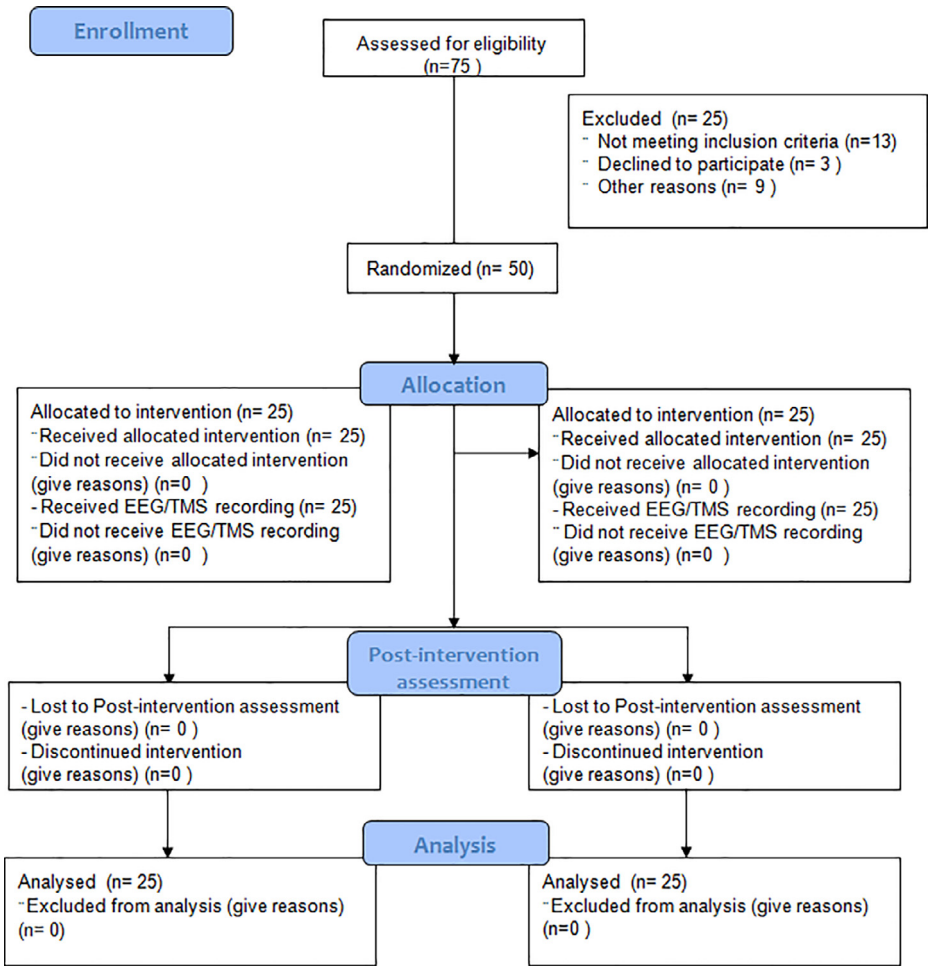

Fig. 2. Experimental study flow diagram.

These oscillations may reflect the ongoing activity related to the motor process characteristics coded into the sensorimotor areas, including kinematics (speeds) and kinetics (motor loads) (Engel and Fries, 2010; Nakayashiki et al., 2014). Moreover, TRCoh offers useful information regarding these sensorimotor events because of the dynamic coupling between different brain areas (including the frontal and sensorimotor regions) (Manganotti et al., 1998; Formaggio et al., 2013). Therefore, the ERS, ERD, and TRCoh data could be important for analysing the recovery mechanisms related to post-stroke brain function recovery (Wu et al., 2015; da Silva and Paz, 2018).

Moreover, since these functional aspects can influence the prognosis and expected outcomes in stroke patients, the analysis of cortical excitability, sensorimotor integration and plasticity probed with TMS has proven useful (Bolognini et al., 2016; Beaulieu and Milot, 2018). It has been shown that corticospinal excitability, as indexed by MEP properties (including integrity degree, latency, magnitude, recruitment curve, and topography mapping) and the sensorimotor integration evaluated using SAI (displaying the inhibitory activity in the perilesional cortex after stroke) play a central role in motor recovery and confirm the long-term functional recovery in humans following a stroke (Clarkson et al., 2010; Paulus et al., 2008; Di Lazzaro et al., 2012; Beaulieu and Milot, 2018; Ferris et al., 2018). Although data on the correlation between cortical inhibition and motor behaviour are still partial (Turco et al., 2018), this study used an SAI assessment, as an important outcome measure because it correlates significantly with movement preparation (Asmussen et al., 2014), the specific digits involved (Asmussen et al., 2014), and functional recovery (Di Lazzaro et al., 2012). In addition, this study's analyses focused on the modulation of plasticity of corticospinal excitability employing rapid, non-invasive, neuromodulation protocol (rPAS). This allowed further investigation of MEP–SAI–behavioral correlation, that is a more extensive assessment of the plasticity of corticospinal excitability and evaluation of the compensatory changes in the contra-lesional hemisphere after stroke in relation to the functional motor outcome and robotic-induced motor-function changes (Kim et al., 2016; Johansson, 2000; Nie and Yang, 2017; Simonetta-Moreau, 2014; Pekna et al., 2012; Weder et al., 2016; Ferris et al., 2018).

2.4.1. EEG analysis

We analysed the EEG results in the time-frequency domain and the TRCoh (functional coupling) between the cortical regions. The EEG recordings were obtained during motor tasks in both the AHT and CHT groups using 21 Ag–AgCl disk-electrodes, positioned according to the international 10/20 system (Micromed; Mogliano Veneto, Treviso, Italy). Two surface electrodes were placed on the flexor radialis carpi muscle to acquire an electromyography (EMG) signal and an EOG channel was also used. The EMG was recorded from this muscle concerning movement onset detection in relation to EEG recording. Impedance was maintained below 10kΩ. The reference was placed on both the mastoids and the ground posterior to Pz. The EEG data were acquired at a rate of 250 Hz. The EEG was then pruned of artefacts (ocular, cardiac,

and scalp muscle) using an independent component analysis procedure, average re-referenced, band-pass filtered at 1–35 Hz (FIR).

Time–frequency power based on continuous wavelet transform (CWT) for 6 s epochs [−1:5] s (0 as the movement onset detected by the EMG signal from the flexor radialis carpi muscle) was computed and averaged among the epochs. After removing artefactual epochs (visible inspection and independent component analysis procedure), the time course of event-related synchronisation (ERS) and desynchronisation (ERD) for each channel–group (affected and unaffected frontal F –F3,F7;F4,F8– affected and unaffected centroparietal CP –C3,P3;C4,P4– affected and unaffected temporal T –T3,T5;T4,T6) was computed according to the formula: $ERS/D = \frac{P_{activation} - P_{rest}}{P_{rest}} \times 100$, where P_{rest} is an average power in reference time [−1:−0.5] s (Müller-Putz et al., 2007), and $P_{activation}$ is the power at each time point of the epoch following movement onset (number of time points: 1250). Consequently, spectral perturbation for the upper α (10–12 Hz) and β (13–30 Hz) frequency range was calculated as the percentage power change over all of the 1250 time points in the grouped channels. The frequency ranges were analysed because movement preparation and execution produce distinct spectral perturbation over the sensorimotor area within a 10–20 Hz range (Leocani et al., 1997).

Electrodes were grouped into the aforementioned channel groups depending on the foremost brain functions associated with motor recovery beneath such electrodes, that is, the actual motor status and the attentional level for frontal electrode-group (approximately over premotor cortex, which is associated with both baseline motor status and recovery gain) (Wu et al., 2015; Calabrò et al., 2018; Lam et al., 2018; Johansen-Berg et al., 2002; Ward et al., 2003; Loubinoux et al., 2003; Wei et al., 2013; Mihara et al., 2013); the basic sensorimotor integration processes for centroparietal electrode-group (related to motor behaviour resulting from precentral, intermediate, caudal, and rostral-postcentral gyri activity) (Homan et al., 1987); and the brain activities related to vocal order recognition and interpretation, depth perception, and attention level for the temporal electrode-group (Noppeney et al., 2006; Allen et al., 2008). Since it is well known that stroke injury can produce both local and network dysfunctions, different groups were selected to investigate not only the loss of local neural function but also the lesion-induced changes in large fronto–temporo–parietal networks (Zou et al., 2018; Zhao et al., 2018).

To obtain TRCoh, we first computed the time–frequency representations of pair-wise channel groups (x, y) in each trial, as well as their squared auto–spectra $|x|^2$ and $|y|^2$ and the cross–spectrum $x \times y$, using CWT. Auto–spectrum expresses the power related to each frequency in a channel; the cross-spectrum estimates the transfer of linear information from one signal to the other and vice-versa). As a consequence, the coherence estimates the amount of the linear information of one signal explained by the other signal, thus estimating the causality between the two signals. In particular, CWT coherence assesses the coherence between two signals whether ergodicity and stationarity assumptions are not respected and enables a time-varying analysis of the coherence.

Then, the estimate of the time–frequency coherence was computed after averaging across trials, according to the formula: $Coh = \frac{|S_{xy}|^2}{S_x S_y}$, where $|S_{xy}|^2$ is the squared magnitude of the cross-spectrum of channel–groups x and y, and S_x and S_y the auto-spectra of such channel-groups (Alia et al., 2017). Thereafter, TRCoh between the channel-group x and y was obtained by subtracting the coherence values during rest from those during activation according to the formula $TRCoh = Coh_{activation} - Coh_{rest}$, where Coh_{rest} is the average Coh in the reference time [−1:−0.5]s, and $Coh_{activation}$ is the Coh at each of the 1250 time points following movement onset (Formaggio et al., 2015). To calculate the spatiotemporal TRCoh between the affected centroparietal channel-group vs. each other channel-group, we calculated the mean TRCoh value from the TRCoh values of the 1250 time points following movement onset (Formaggio et al., 2015). The TRCoh increments and decrements from rest to activation for each channel comparison correspond to increments and decrements in Coh, respectively.

2.4.2. TMS procedures

To probe the corticospinal excitability, monophasic TMS pulses were first delivered to both the affected and unaffected M1 using a 9 cm standard figure–of–eight coil wired to a high–power Magstim 200^2 stimulator (Magstim Company; Whitland, Dyfed, UK). We identified the optimal position for left and right abductor pollicis brevis muscle (APB) activation by shifting the coil position in steps of 0.5 cm around the presumed M1-HAND. The coil position, at which the largest MEP with the steepest initial slope in the relaxed APB muscle was evoked by single TMS stimuli, was marked with a pen as the "hot spot". The handle of the coil pointed backwards and laterally away from the midline at a 45° angle and was thus approximately perpendicular to the line of the central sulcus. The coil current flowed toward the handle during the rising phase of the magnetic field. Thus, the induced current had a posterior–to–anterior direction flow in the cortex. The rise time of the monophasic magnetic stimulus was ∼100 μs, decaying back to zero in ∼800 μs. We provided single–pulse TMS at an intensity sufficient for evoking a 0.5 mV peak–to–peak MEP amplitude in the relaxed right and left APB (corresponding to ∼115% of the resting motor threshold, that is the minimum intensity that evoked a peak–to–peak MEP of 50 μV in at least 5 out of 10 consecutive trials in the relaxed APB muscle). The setup employed was safe and comfortable for the patients and sufficient to evoke MEP in all of the patients. Excitation of the neighbouring cortical regions was minimised by avoiding of high TMS intensities, thus minimising potential floor or ceiling effects during excitability assessments, and excluding the necessity of pre-activation, motor imagery, or both to elicit MEPs (Quartarone et al., 2006; Tolmacheva et al., 2017; Palmer et al., 2018). Approximately 20 single–pulse stimuli per hemisphere were delivered to obtain a steady MEP amplitude.

SAI was tested from both the hemispheres according to the Tokimura paradigm (Tokimura et al., 2000). A transcranial magnetic test stimulus (evoking an MEP of approximately 0.5 mV from the relaxed APB) given to the M1 was preceded by an electrical conditioning stimulus administered to the contralateral median nerve at the wrist (through bipolar electrodes, with the cathode placed proximally). Electric stimuli consisted of square-wave pulses (pulse-width of 500 μs) with an intensity sufficient for evoking minimal activation of the APB muscle. In each individual, the interstimulus interval between the conditioning (electric) and test (magnetic) stimuli was equal to the latency of the N20 component of the somatosensory evoked potentials +5 ms. At least 15 paired electric-magnetic stimuli (that is, SAI) randomly intermingled with at least 15 unconditioned magnetic stimuli (that is, MEP alone) were recorded. In general, approximately 20 single- or paired-pulse stimuli per hemisphere were used to obtain a steady conditioned or unconditioned MEP. The mean amplitude of the conditioned MEP (paired stimuli) was expressed as a percentage of the mean amplitude of the unconditioned MEP (i.e., MEP alone). The strength of SAI was expressed by the amplitude reduction induced by the peripheral stimulus. The trials were removed from the analysis if the APB muscle was not fully relaxed. The electrical stimuli were generated by a Digitimer D–160 stimulator (Digitimer Ltd, Welwyn Garden City, Hertfordshire, UK).

This study assessed the corticospinal excitability following the rPAS session. This consisted of 600 pairs of stimuli delivered to the affected M1 at 5 Hz for 2 min (Quartarone et al., 2006). Each pair of stimuli was composed of a biphasic TMS stimulus (with a pulse width of ~300 μs; the MEP amplitude was recorded from the affected APB muscle at rest) delivered to the affected M1 through a Magstim Rapid stimulator (Magstim Company, Whitland, Dyfed, UK), which was preceded by an electrical conditioning stimulus administered to the contralateral median nerve (with a pulse width of ~300 μs). The inter–stimulus interval was individually adapted to the latency of the N20 component of somatosensory evoked potentials +5 ms. It has been shown that such an inter-stimulus interval at low frequency produce a long–lasting facilitation of motor cortical excitability (Wolters et al., 2003). The electrical stimulus intensity was twice that of the sensory threshold, while the TMS-stimulus intensity was 90% of the active motor threshold (from affected APB muscle) in each individual. The active motor threshold is defined as the minimum intensity that produces MEPs of 100 μV peak–to–peak amplitude in at least three out of five single-pulse trials. The intensities of the peripheral and transcranial stimuli were always at the subthreshold for eliciting muscle twitches to avoid any conditioning effect related to re-afferent feedback activation, to avert elicitation of the descending volleys (Di Lazzaro et al., 1998), and to minimise the excitation of the neighbouring cortical regions (Takano et al., 2004). The overall change in the MEP amplitude and SAI strength from both of the hemispheres as compared to baseline (TPRE) was calculated by dividing the maximal for the mean value of MEP and SAI recorded immediately (T0), 30 min (T30) and 60 min (T60) after rPAS application. Such overall changes were obtained as measure of the corticospinal excitability and sensorimotor plasticity.

2.5. Sample size

A sample size of 40 subjects, 20 in each arm, was estimated as sufficient to detect a pre-post treatment difference of 20% in the primary outcomes (corresponding to the minimal clinically important difference of both the outcome measures), assuming a standard deviation of 1.917 using a two-tailed *t*-test of difference between means (Kwakkel et al., 2008a, 2008b; Beebe and Lang, 2009; Arya et al., 2011; Lum et al., 2012; Chang and Kim, 2013; Woytowicz et al., 2016; Yue et al., 2017), with $\alpha = 0.05$ and $1 - \beta = 0.95$. Considering a dropout rate of 10% the sample size required was rounded–up to 50 (25 per group).

2.6. Randomization

The patients were randomised into the AHT or CHT group with a 1:1 allocation ratio. Sealed envelopes marked on the inside with a +(AHT) or −(CHT) were prepared in advance.

2.7. Blinding

The patient allocation was blinded for the researchers and the therapists who analysed the data and performed the clinical tests.

2.8. Statistical methods

All of the randomized patients were included in the primary analysis, as an intent-to-treat approach was adopted. Descriptive statistics were presented for all of the outcomes for both interventions (with pre-post changes), including the effect size measures between the two independent groups. Cohen's d calculation size and the 95% confidence interval are both reported. The effect size relevance was thresholded poor at ≤0.2, moderate at <0.5, large at <0.8 and very large at ≥0.9 (Cohen, 1988; Rosenthal, 1996).

The Kolmogorov–Smirnov test estimated the distribution of data. All of the data were normally-distributed ($p > 0.2$). For each outcome, the equivalence between the two groups, at baseline, was evaluated using the *t*–test. The treatment effect on the clinical and TMS outcomes was subjected to repeated-measures ANOVA with the *group* as the between-subjects factor (two levels: AHT and CHT) and the *time* as the within-subject factor (two levels: PRE and POST). Statistical significance was set at $p < 0.05$. *Post–hoc* paired *t*–tests (Bonferroni corrected) were carried out to determine the location of any important difference between time points in the presence of significant main effects.

Each TRCoh for α and β frequency ranges of the affected CP vs. each other channel–group was subjected to repeated–measures ANOVA with *group* as between–subjects factor (two levels: AHT and CHT) and *time* as within–subject factor (two levels: PRE and POST). Statistical significance was set at $p < 0.05$. *Post-hoc* paired *t*-tests were done with multiple comparisons correction (Bonferroni correction).

Paired–sample two–tailed *t*–tests were calculated to determine the significant differences between the ERD and ERS values, in the α and β ranges at each of the 1250 time points, and a reference condition (when the power computed at rest is equal to the power computed during the active condition) of each electrode–group and for pre–post comparison (Formaggio et al., 2008, 2013).

Finally, Pearson's correlation coefficient was carried to assess the correlation between the clinical and electrophysiological parameters.

3. Results

3.1. Participant flow, recruitment, and baseline data

A total of 75 patients were screened for eligibility and 50 met the eligibility criteria and were randomised between January and February 2018 (Fig. 1). The baseline demographics (Table 1), clinical and TMS characteristics (Table 2) were similar in of the both groups (see the *t*–test *p*–values). All of the patients showed low MEP amplitude and a low SAI in the affected side, paralleled by a high SAI in the unaffected side, without group differences. MEP and SAI from both of the hemispheres were measured after boosting sensorimotor plasticity using rPAS. At baseline, the response to rPAS was overall small and characterised by an MEP amplitude and an SAI increase in the affected side and SAI decrease in the unaffected hemisphere, without group differences. The MEP amplitude in the unaffected side was unchanged (Table 2).

A reduced α TRCoh was found between the affected CP electrodes and both the affected F and unaffected CP electrodes. A reduced β TRCoh was also between the affected CP electrodes and both the affected and unaffected F electrodes. In parallel, both of the groups showed a deterioration in α and β ERD at the movement onset in the affected F electrodes and in the sequential ERS within the affected CP electrodes.

3.2. Analyses and primary outcomes

All of the randomised patients completed the trial without any adverse events, and the data were thus analysed (Fig. 1).

At the end of the training, both of the groups showed significant clinical improvement (FMAUE and 9HPT, $p < 0.001$) (Table 2). However, the AHT group had a significantly higher FMAUE score and lower 9HPT completion time than the CHT group (both $p < 0.001$) (Table 2). Specifically, AHT induced a very large 9HPT decrease ($d = 0.9$), whereas the same effect in CHT was moderate–to–large ($d = 0.6$) (Table 2). Consequently, a very significant group difference ($d = 0.9$) was found. AHT induced a large FMAUE increase

Table 2
This shows PRE and POST mean (s.d.) values of primary (clinical) and secondary (transcranial magnetic stimulation) outcomes, *t*-test between groups at entry time (*), *time* effect of repeated measures ANOVA, with *d* effect size with 95% CI of within– and between–group POST-PRE differences, and interaction effect (*time* × *group*) of repeated measures ANOVA (with *post-hoc p*-values).

Parameter		PRE		*p*-value*	POST		Time effect $F_{(1,48)}$,p,η^2	POST-PRE *d* (95%CI)			Interaction effect (*time* × *group*) $F_{(1,48)}$,p,η^2	*Post-hoc p*-value		
		AHT	CHT		AHT	CHT		AHT	CHT	AHT-CHT		AHT	CHT	AHT-CHT
9HPT(s)		63(7)	64(5)	0.5	46(5)	55(6)	59,<0.001,0.9	0.8(−0.8;2.4)	0.6(−1.2;2.3)	0.9(−1.3;1.5)	42,<0.001,0.9	<0.001	<0.001	<0.001
FMAUE		29(3)	30(3)	0.8	36(4)	34(4)	23,<0.001,0.8	0.7(−2.8;1.5)	0.5(−2.5;1.5)	0.9(0.5;1.2)	29,<0.001,0.9	<0.001	<0.001	<0.001
MEP_aff (mV)		0.4(0.1)	0.41(0.1)	0.9	0.56(0.5)	0.48(0.5)	8.2,0.006,0.8	0.8(−2.8;2.8)	0.5(−0.6;−0.5)	0.9(0.9;0.96)	18,<0.001,0.9	<0.001	<0.001	<0.001
MEP_unaff (mV)		0.91(0.1)	0.92(0.1)	0.8	0.9(0.1)	0.89(0.1)	p = 0.7	0.05(0.02;0.07)	0.1(0.11;0.17)	0.1(0.09;0.11)				
SAI_aff (%)		56(6)	57(7)	0.9	67(7)	62(7)	50,<0.001,0.9	0.4(−2.5;1.3)	0.1(−2.1;1.4)	0.9(0.6;1.2)	52,<0.001,0.9	<0.001	<0.001	<0.001
SAI_unaff (%)		70(8)	68(7)	0.7	50(6)	56(7)	21,<0.001,0.9	0.8(−1;2)	0.6(−1.2;2.5)	0.9(0.2;1.7)	15,0.001,0.8	<0.001	<0.001	<0.001
rPAS	MEP_aff (%)	109(12)	104(11)	0.1	130(15)	106(12)	46,<0.001,0.9	0.6(−4.2;3)	0.1(−3.1;3.3)	0.9(0.2;1.7)	104,<0.001,0.9	<0.001	0.2	<0.001
	MEP_unaff (%)	101(11)	100(11)	0.3	99(11)	99(11)	p = 0.7	0.1(−3;3.1)	0.05(−3;3)	0.1(0.9;1.1)				
	SAI_aff (%)	111(13)	105(12)	0.6	120(14)	106(12)	94,<0.001,0.9	0.3(−3.8;3.2)	0.04(−3.1;3.2)	0.7(0.6;1.2)	7.1,0.01,0.7	0.003	0.2	<0.001
	SAI_unaff	70(8)	72(9)	0.5	56(7)	65(9)	97,<0.001,0.9	0.7(−1.2;2.6)	0.4(−1.7;2.5)	0.9(0.4;1.4)	12,0.001,0.8	<0.001	0.4	<0.001

Legend: FMAUE Fugl-Meyer Assessment for Upper Extremity, 9HPT Nine-Hole Peg Test, MEP motor evoked potential, SAI short-latency afferent inhibition, _unaff unaffected hemisphere, _aff affected hemisphere, rPAS repetitive paired associative stimulation, AHT Amadeo™ hand training, CHT conventional hand training).

(d = 0.7), whereas the same effect in CHT was moderate (d = 0.5). Furthermore, a considerable group difference (d = 0.9) was also detected (Table 2).

3.2.1. Training effects on secondary outcomes: TMS and DGF

Both of the groups showed significant TMS changes, with the exception of MEP amplitude from the unaffected hemisphere both before and after rPAS application (see *time* effect in Table 2). However, the AHT group had significantly higher MEP amplitude from the affected hemisphere and SAI magnitude from both of the hemispheres, both before and after rPAS application, than the CHT group (see the interaction effect in Table 2).

Both of the groups showed no significant effects on MEP amplitude in the unaffected hemisphere (p = 0.7).

Both of the groups showed significant MEP amplitude increase in the affected hemisphere (p = 0.006), but the AHT group had significantly higher MEP than the CHT group (p < 0.001). AHT had an important effect on MEP amplitude in the affected hemisphere (increase) (d = 0.8), whereas the same effect in CHT was moderate (d = 0.5). A considerable difference was also found between the effects on the two groups regarding MEP amplitude increase in the affected hemisphere (d = 0.9) (Table 2).

Both of the groups showed significant SAI increase in the affected hemisphere (p < 0.001), but the AHT group had significantly higher SAI than the CHT group (p < 0.001). The AHT had a moderate effect on SAI (increase) in the affected hemisphere (d = 0.4), whereas the same effect in the CHT was poor (d = 0.1) (Table 2). Hence, a very large difference was found between the effects of the two treatments on SAI in the affected hemisphere (d = 0.9).

Both of the groups showed a relevant SAI decrease in the unaffected hemisphere (p < 0.001), but the AHT group had a notably higher SAI than the CHT group (p = 0.001). The AHT had a substantial effect on SAI in the unaffected hemisphere (decrease) (d = 0.8), whereas the same effect in the CHT was moderate–to–large (d = 0.6). However, a very large difference was found between the effects of the two groups on SAI in the unaffected hemisphere (d = 0.9) (Table 2).

Regarding the rPAS aftereffects after the training, both of the trainings had a poor effect on the rPAS–induced MEP amplitude decrease in the unaffected side (p = 0.7).

Both of the groups showed an important rPAS–induced MEP amplitude increase in the affected side (p < 0.001), but the AHT group had significantly higher MEP than the CHT group (p = 0.001). The AHT group showed a moderate–to–large effect on rPAS–induced MEP amplitude increase in the affected side (d = 0.6), whereas the same effect in the CHT was poor (d = 0.1). In fact, a very large difference was observed between the effects of the two groups regarding MEP amplitude increase in the affected side (d = 0.9).

Both of the groups showed an appreciable rPAS–induced SAI decrease in the unaffected hemisphere (p < 0.001), but the AHT group had a significantly lower SAI than the CHT group (p = 0.001). The AHT had a substantial effect on the rPAS–induced SAI decrease in the unaffected hemisphere (d = 0.7), whereas the same effect in the CHT was moderate (d = 0.4). Hence, a very large difference was found between the effects of the two treatments concerning SAI decrease in the unaffected hemisphere (Table 2).

Although both of the groups showed significant rPAS–induced SAI increase in the affected hemisphere (p < 0.001), the AHT group had a significantly higher MEP than the CHT group (p = 0.01). AHT had a moderate effect on rPAS–induced SAI increase in the affected hemisphere (d = 0.3), whereas the same effect in CHT was poor (d = 0.04). However, a moderate difference was found between the effects of the two groups concerning SAI increase in the affected hemisphere (d = 0.7) (Table 2).

The DGF, which was measurable only in the patients in the AHT group, had significantly decreased from 80(10) to 45(8)%, with a large–to–very large effect (d = 0.8; −1.84 to 3.58) (*time* effect $F_{(1,24)} = 48$, $p < 0.001$, $\eta^2 = 0.9$).

3.2.2. Training effects on secondary outcomes: TRCoh

Both of the groups showed relevant α and β TRCoh changes, with the exception of β TRCoh between unaffected F and affected CP. The AHT group had a significantly high β TRCoh between unaffected F and CP, which was not the case of the CHT group.

Specifically, both of the groups showed a noteworthy increase in α TRCoh between the affected CP and F (*time* effect $F_{(1,48)} = 15$, $p < 0.001$, $\eta^2 = 0.9$). However, the AHT group had much higher Coh values than the CHT group (*time* × *group* interaction $F_{(1,48)} = 14$, $p < 0.001$, $\eta^2 = 0.9$). The AHT had a moderate effect on Coh (d = 0.4; 0.26–0.54), the effect of CHT on Coh (d = 0.2; 0.13–0.27) was poor producing a subsequent between-group difference (d = 0.9; 0.58–1.22).

Both of the groups demonstrated a significant increase in α TRCoh between affected and unaffected CP (*time* effect $F_{(1,48)} = 9$, $p = 0.004$, $\eta^2 = 0.8$), while the AHT group had significantly higher Coh values compared to the CHT group (*time* × *group* interaction $F_{(1,48)} = 58$, $p < 0.001$, $\eta^2 = 0.9$). While AHT showed a considerable effect on Coh (d = 0.9; 0.57–1.19), the effect of CHT was moderate (d = 0.3; 0.19–0.41), with a consequent very large between-group difference (d = 0.9; 0.61–1.29).

A significant increase in β TRCoh between affected CP and F (*time* effect $F_{(1,48)} = 5.7$, $p = 0.02$, $\eta^2 = 0.6$) was seen in both of the groups. The AHT group had significantly higher Coh values than the CHT group (*time* × *group* interaction $F_{(1,48)} = 10$, $p = 0.002$, $\eta^2 = 0.9$). Thus, the AHT had a very large effect on Coh (d = 0.9; 0.59–1.23), whereas the effect of the CHT was moderate (d = 0.5; 0.32–0.68), with a consequent large between-group difference (d = 0.8; 0.52–1.08).

β TRCoh was significantly increased between the unaffected F and affected CP (*time* effect p = 0.5; *time* × *group* interaction $F_{(1,48)} = 9.3$, $p = 0.004$, $\eta^2 = 0.9$) only in the AHT group with a consistent effect on Coh (d = 0.9; 0.58–1.22). The effect of the CHT was poor (d = 0.05; 0.02–0.07) with a consequent large between-group difference (d = 0.8; 0.5–1.04).

As shown in Fig. 3, α TRCoh between the affected CP and F electrodes showed a larger increase following AHT compared to CHT (*time* × *group post-hoc t*-test AHT $p < 0.001$, CHT $p = 0.003$; between–group $p < 0.001$). Similarly, α TRCoh between the affected CP and the unaffected CP electrodes increased more following AHT compared to CHT (*time* × *group post-hoc t*-test AHT $p = 0.008$, CHT $p = 0.01$; between–group $p < 0.001$). In parallel, β TRCoh between the affected CP and F electrodes showed a greater increase following AHT compared to CHT (*time* × *group post-hoc t*-test AHT $p < 0.001$, CHT $p = 0.01$; between–group $p < 0.001$). Finally, β TRCoh between the affected CP and the unaffected F electrodes showed an increase following AHT compared to CHT (*time* × *group post-hoc t*-test AHT $p < 0.001$, CHT $p = 0.4$; between–group $p < 0.001$).

3.2.3. Training effects on secondary outcomes: brain oscillations

Both of the hand trainings disturbed the α and β rhythms within F and CP electrode-groups of both of the hemispheres. As indicated by the ERS and ERD *t*–map in Fig. 4, the AHT strengthened the α–β ERD ($t_{(24)} = -16$, $p < 0.001$) within the affected F electrodes, the α ERS ($t_{(24)} = 24$, $p < 0.001$) and β ERD ($t_{(24)} = -15$, $p < 0.001$) within the affected CP electrodes, and the α–β ERS over the unaffected F electrodes ($t_{(24)} = 15$, $p < 0.001$).

The CHT strengthened the α–β ERD ($t_{(24)} = -15$, $p < 0.001$) over the affected F electrodes, α ERD ($t_{(24)} = -23$, $p < 0.001$) and β ERS ($t_{(24)} = 11$, $p < 0.001$) within the affected CP electrodes, whereas

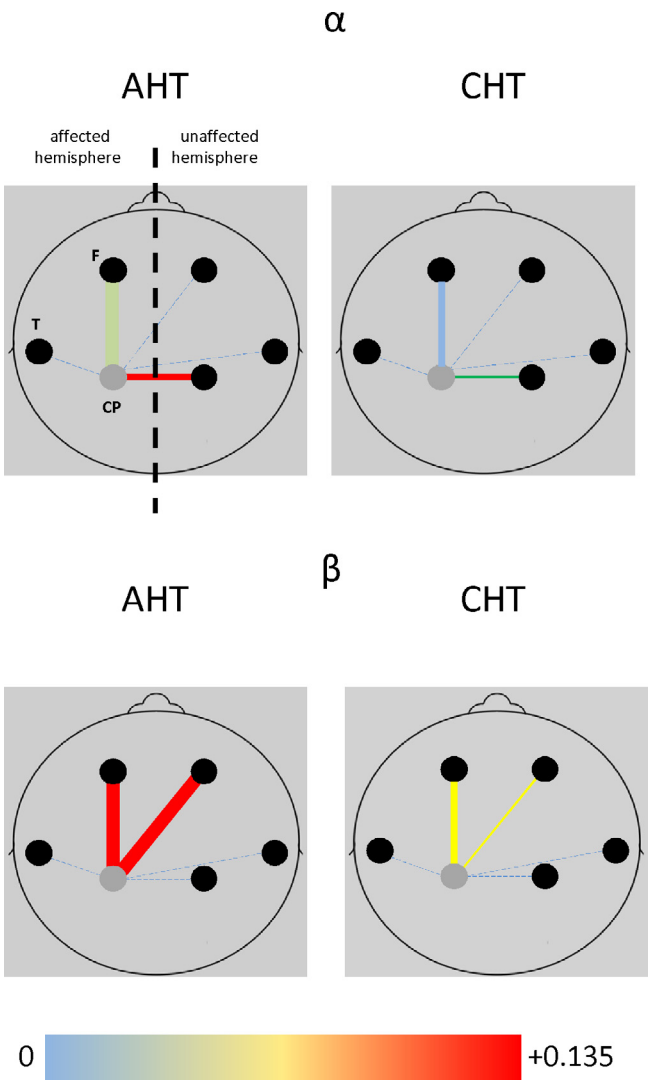

Fig. 3. Grand average of the topographic task-related coherence (TRCoh) maps in the upper α (10–12 Hz) and β (13–30 Hz) frequency ranges. The dots indicate the electrode positions (frontal, F, centroparietal, CP, and temporal, T, groups), and the affected hemisphere is plotted on the left. The affected CP channel-group is marked in grey as mean TRCoh values were thus calculated between the affected CP vs. each other channel-group. The colour-coded lines show the magnitude of the TRCoh changes, with warm colours indicating an increase in TRCoh (functional coupling) and cold colours representing no changes in TRCoh (decoupling). The significance of the within-group TRCoh changes is shown by the thickness-coded lines, with thick lines $p < 0.001$, mild lines $0.001 < p < 0.01$, thin lines $0.01 < p < 0.05$, and dotted lines $p > 0.05$. (For interpretation of the references to colour in this figure legend, the reader is referred to the web version of this article.)

there were no effects within the unaffected F and CP electrodes (Fig. 4).

Therefore, the clear-cut differences between the two groups consisted of a greater α ERD within the affected CP electrodes ($t_{(48)} = -7.8$, $p < 0.001$), a greater β ERD within the affected F electrodes ($t_{(48)} = -7.6$, $p < 0.001$), and a slightly greater α and β ERS within the unaffected F electrodes ($t_{(48)} = -2.2$, $p = 0.03$) in the AHT as compared to the CHT.

3.3. Clinical-electrophysiological correlations

Clinical improvement was paralleled by some electrophysiological changes. In particular, a more evident clinical improvement (estimated with the combined primary outcomes) was achieved when SAI in the affected hemisphere increased ($R^2 = 0.698$,

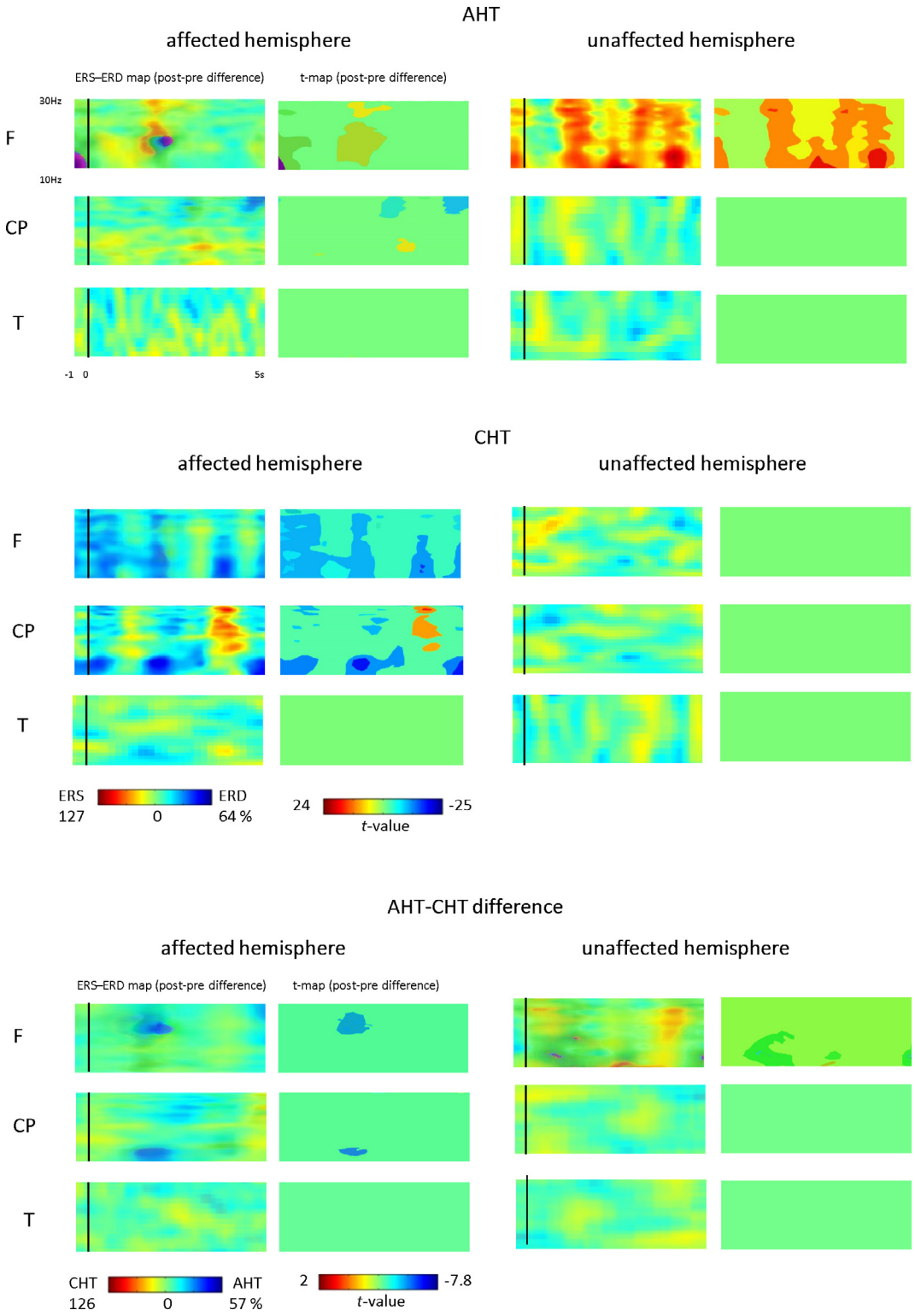

Fig. 4. POST-PRE differences in the grand average maps of the event-related spectral perturbations (event-related desynchronisation, ERD, and synchronisation, ERS) (left sub-columns) and of grand average *t*-maps (right sub-columns) in the 10–30 Hz range within the frontal, F, and centroparietal, CP, and temporal, T, channel-groups of both the hemispheres, following the Amadeo™ hand training (AHT) and conventional hand training (CHT) groups. The post-pre AHT-CHT differences at the end of the trainings are plotted, as well, at the bottom of the figure. The vertical black line denotes movement initiation.

$p < 0.001$), rPAS aftereffects in the unaffected hemisphere decreased ($R = -0.7662$, $p < 0.001$), and F–CP α TRCoh in the unaffected hemisphere increased ($R = 0.8281$, $p < 0.001$), which mainly involved the patients who practiced AHT (Fig. 5). Moreover, the decrease in the rPAS aftereffects within the unaffected hemisphere, the increase in the rPAS aftereffects within the affected hemisphere, and the strengthening of F–CP β TRCoh within the unaffected hemisphere were significantly correlated ($r = 0.904$, $p < 0.001$).

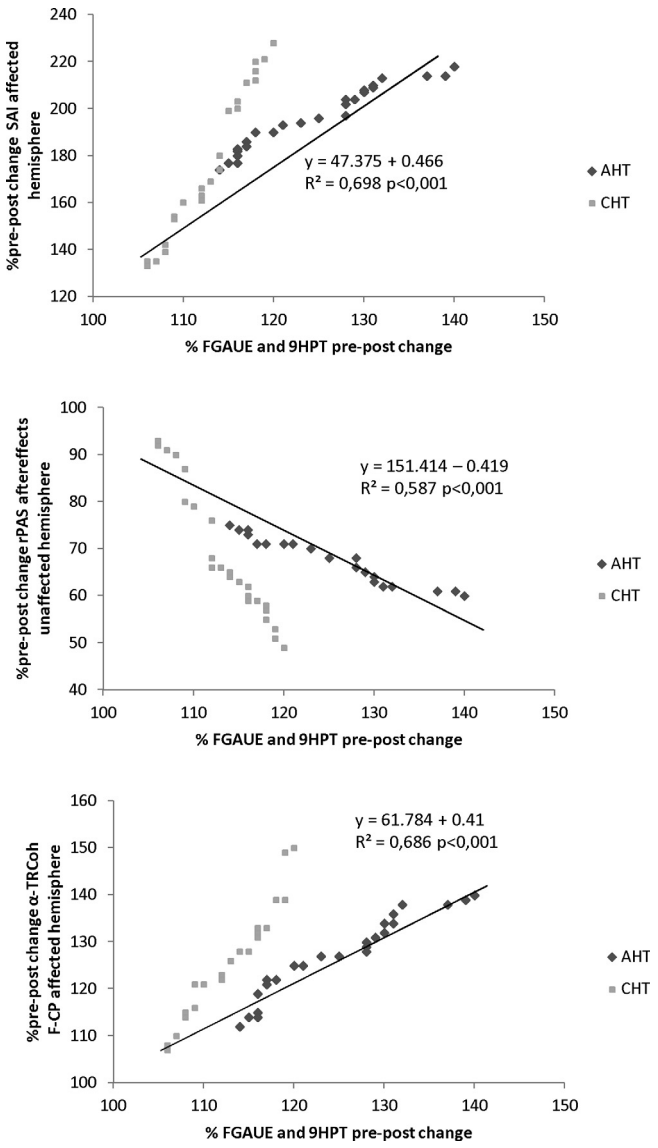

Fig. 5. Scatterplots of the clinical-electrophysiological correlations. The x-axis indicates the pre-post clinical improvement (composite primary outcome). The y-axis indicates the pre-post electrophysiological changes, which were more evident from practising Amadeo™ hand training (AHT) than conventional hand training (CHT).

4. Discussion

Growing evidence supports the usefulness of intensive, repetitive, and task-oriented robot-guided rehabilitation of the upper limb to promote motor re-learning and minimise motor deficit (Kwakkel et al., 2008a, 2008b; Krebs and Volpe, 2013; Norouzi-Gheidari et al., 2012; Sivan et al., 2011; Pollock et al., 2014). However, there is little information regarding the usefulness of hand robotic specific rehabilitation (Kwakkel et al., 2008a, 2008b; Mehrholz et al., 2008; Balasubramanian et al., 2010). Our data indicate that hand robotics using Amadeo™ had positive effects on the upper extremity function in patients with chronic stroke (Sale et al., 2012, 2014). As additional descriptive data, both of the groups recognised an amelioration in Functional Independence Measure scoring. However, the patients who underwent the AHT showed greater improvement in self-care and transfers sub-items than those who practiced the CHT.

Although the clinical improvements were substantial in both of the groups, they were more evident following AHT than CHT. The novelty of this study consists of the provision of putative neurophysiological mechanisms supporting the greater strength of robot-aided hand training (using Amadeo™) for achieving clinical improvement, as compared to an equivalent dose of conventional physical hand training. Robotic hand training stimulated a more evident reshaping of movement-related brain oscillations and connectivity, and a stronger rebalance of the mechanisms of sensorimotor integration and plasticity of corticospinal excitability between the affected and unaffected hemispheres. Better clinical improvement was accomplished when SAI in the affected hemisphere was weak (that is, percentual increase) and SAI in the unaffected hemisphere was strong (that is, percentual decrease). The MEP and SAI changes induced by rPAS were greater in the affected than unaffected hemisphere and F–CP α TRCoh in the affected hemisphere were high. This scenario was more evident in the patients who practiced AHT as compared to those who underwent CHT.

Therefore, robot-aided and conventional hand training used the same neurophysiological mechanisms subtending motor recovery, which were augmented following AHT compared to CHT. This difference may be related to the strengthening of the frontoparietal connectivity (β TRCoh modulation) and frontal β power within the unaffected hemisphere, which was the distinctive feature between the two treatments (that is, obtained using only AHT). A higher frontoparietal activation within the unaffected hemisphere paralleled a more efficient interhemispheric information transfer, as suggested by the rebalance of the interhemispheric mechanisms of sensorimotor integration (reciprocal modulation of the magnitude of SAI between the two hemispheres) and the plasticity of the corticospinal excitability (reciprocal modulation of the magnitude of MEP between the two hemispheres, and strengthening of rPAS aftereffects in the affected hemisphere, paralleled by a toning-down in the unaffected hemisphere). This is persistent with the principle of interhemispheric plasticity, a key issue in renewing both simple and complex motor activities, thus favouring motor function recovery (Takeuchi et al., 2012a, 2012b; Alia et al., 2017; Borich et al., 2018; Manganotti et al., 1998; Di Pino et al., 2014; Nudo, 2013). Specifically, restoring interhemispheric balance by reducing transcallosal inhibition, by providing the patients with intensive and repeatable robot–aided training exercises, is important for limiting use-dependent alterations in interhemispheric connectivity and preventing maladaptive plasticity (Takeuchi and Izumi, 2013), as well as removing the "plasticity brakes" exerted by perilesional or lesional tissues (Kwakkel et al., 2008a, 2008b; Spalletti et al., 2017; Johansson, 2011).

The closely correlated changes in frontoparietal connectivity, sensorimotor integration, and interhemispheric plasticity provided by robotic rehabilitation may depend on a "bottom–up" and/or a "top–down" mechanism. Traditional rehabilitation approaches, robotic technologies, and mechatronic devices can be qualified as "bottom–up" approaches, that is, they act at the bodily level (bottom) to influence the neural system (top), harnessing the mechanisms of neural plasticity (Krebs et al., 2009). One may argue that task–specific training alone is more likely to enhance behavioural compensation than effective motor recovery. Accordingly, these devices have been modelled to carry out task-oriented motor exercises. In addition they have been equipped with "enriched environments" to augment the generalising effect of spontaneous biological recovery instead of promoting compensation strategies (as in the case of Amadeo™), for a "top–down" approach (Prieto et al., 2014; Chisari, 2015). Therefore, there could be a stronger fronto-parietal, "top–down" control from high–order to the primary sensorimotor areas (as indicated by the bilateral involvement of the frontal electrodes concerning α and β power and TRCoh

modulation), which both facilitates the plasticity mechanisms of motor learning within the affected hemisphere and reverts the compensatory, but maladaptive, plasticity mechanisms within the unaffected hemisphere. However, there could be a "bottom–up", direct involvement of the sensorimotor integration mechanisms likely due to a greater amount of sensory and proprioceptive information coming from robotic device and its visuomotor feedback, with a secondary involvement of the frontoparietal networks. Both of these mechanisms may have contributed to avoid the exacerbation of the use-dependent plasticity impairment within the affected hemisphere due to the abnormally increased interhemispheric inhibition following stroke by modifying the frontoparietal connections (Kwakkel et al., 2008a, 2008b; Allred et al., 2010).

The specific strengthening of frontoparietal connectivity and power within the unaffected hemisphere provided by AHT may depend on the more intense, frequent, repeatable, focused on distal segments, and task-oriented motor exercises provided by robotic–hand devices (Formaggio et al., 2013; Ramos-Murguialday and Birbaumer, 2015; Yue et al., 2017; Hatem et al., 2016). Conjugating hand therapy exercises performed more repetitively, consistently, and longer, with high focus on rehabilitative training on the hand may boost specific types of neuroplasticity mechanisms (including a more evident and specific network perturbation, that is, oscillatory activity and functional connectivity). Moreover, robotic devices either assist or correct the user's movements, thus simultaneously managing the activation of efferent motor and afferent sensory pathways during training (Chisari, 2015). In this way, higher motor function recovery can be obtained (Lo, 2012; Balasubramanian et al., 2010; Lum et al., 2012), as also shown by our data. AHT may also reduce the compensatory hyper-reliance on the proximal paretic side and trunk movements to perform hand motor tasks, usually observed in post-stroke (Roby-Brami et al., 2003), better than CHT.

Some researchers have hypothesized that robotic training may induce a long-lasting reorganisation of such processes through long-term potentiation phenomena at the synaptic and network level within the sensorimotor circuitries determined by intrinsic properties of motor practise (Formaggio et al., 2013; Ramos-Murguialday and Birbaumer, 2015; Kaehlin-Lang et al., 2002; Fazekas et al., 2006; Boscolo Galazzo et al., 2014). A bilateral involvement of the sensorimotor areas has been reported during tasks involving the limb proximal muscles (Nirkko et al., 2001). It is noteworthy that Amadeo™ induced a bilateral involvement in tasks involving the limb distal muscles. Such a bilateral activation could be due to both the motor task employed (Manganotti et al., 1998) and the disease model. These brain activations usually occur during movement planning and execution related to passive, active, and mirror movements (Jang et al., 2004; Matteis et al., 2003). It has been argued that robotic hand devices entrain similar neural circuits regarding passive, active, and imaginary movements, with some distinctive feature (Alegre et al., 2002). In particular, Amadeo™ offers attention–drawing visual feedback (that is, a scheme of the performed movement). Therefore, the entrainment of the mirror system network involved in movement planning and execution via robot-aided hand training may sustain this bilateral frontal activation (Neuper et al., 2005; Stippich et al., 2002; Jang et al., 2004; Matteis et al., 2003), with a prevalence in the unaffected hemisphere, possibly due to the concurrent interhemispheric imbalance following stroke (Seo et al., 2018; Bartur et al., 2018; Pool et al., 2018). This issue is of key importance, as demonstrated by studies focusing on the effects of passive and mirror movement therapy on stroke recovery (Jang et al., 2004; Matteis et al., 2003). Moreover, the potentiation of frontoparietal networks could facilitate patients' mental practise of hand exercises before and/or after physical therapy (Liu et al., 2014), thus further enhancing motor recovery as compared to stand–alone CHT.

Regarding the study limitations, all of the patients were evaluated only at end of the study, and we do not have all of data on the short and long-term follow-up. However, eight patients who were trained with Amadeo™ returned for a follow-up visit after three months, and five had maintained some clinical improvement, whereas six patients who underwent the CHT returned for a follow-up visit after three months, and two of them had retained some clinical improvement. These numbers do not allow the formulation of any conclusions, and whether Amadeo™ has long-lasting aftereffects still must be verified. In addition, other adjunctive measures could have aided in clarifying the neurophysiological mechanisms underlying robot-aided motor recovery (for example, finger muscle representational mapping and the input-output recruitment curve).

In conclusion, although the results of this study are preliminary, Amadeo™ seems to be very promising as an initiator of functional movements in stroke patients. Moreover, these report's findings offer new insights into the role of sensorimotor oscillations and connectivity concerning motor function recovery following robotised hand training. Thus, it is possible to acquire some useful neurophysiological information on the plasticity-based recovery mechanisms after brain injury and following rehabilitation paradigm, so as to refine patient-tailored (that is, highly personalised) rehabilitative paradigm following stroke.

Acknowledgments

We would like to thank the Elsevier Language Editing Services, Prof. Maria Concetta Tripoli, and Prof. Richard Kingsley for having revised the English language.

Conflict of interest

None of the authors has conflict of interest.

Ethical approval

All procedures performed in studies involving human participants were in accordance with the ethical standards of the institutional and/or national research committee and with the 1964 Helsinki declaration and its later amendments or comparable ethical standards.

Funding

No funding to report.

References

Alegre M, Labarga A, Gurtubay IG, Iriarte J, Malanda A, Artieda J. Beta electroencephalograph changes during passive movements: sensory afferences contribute to beta event-related desynchronization in humans. Neurosci Lett 2002;331:29–32.

Alia C, Spalletti C, Lai S, Panarese A, Lamola G, Bertolucci F, Vallone F, Di Garbo A, Chisari C, Micera S, Caleo M. Neuroplastic changes following brain ischemia and their contribution to stroke recovery: novel approaches in neurorehabilitation. Front Cell Neurosci 2017;11:76.

Allen P, Mechelli A, Stephan KE, Day F, Dalton J, Williams S, et al. Fronto-temporal interactions during overt verbal initiation and suppression. J Cogn Neurosci 2008;20:1656–69.

Allred RP, Cappellini CH, Jones TA. The "good" limb makes the "bad" limb worse: experience-dependent interhemispheric disruption of functional outcome after cortical infarcts in rats. Behav Neurosci 2010;124(1):124–32.

Alt Murphy M, Willen C, Sunnerhagen KS. Kinematic variables quantifying upper-extremity performance after stroke during reaching and drinking from a glass. Neurorehabil Neural Repair 2011;25:71–80.

Arya KN, Verma R, Garg RK. Estimating the minimal clinically important difference of an upper extremity recovery measure in subacute stroke patients. Top Stroke Rehabil 2011;18(Suppl. 1):599–610.

Asmussen MJ, Zapallow CM, Jacobs MF, Lee KG, Tsang P, Nelson AJ. Modulation of short-latency afferent inhibition depends on digit and task-relevance. PLoS One 2014;9(8):e104807.

Balasubramanian S, Klein J, Burdet E. Robot-assisted rehabilitation of hand function. Curr Opin Neurol 2010;23(6):661–70.

Bartur G, Pratt H, Frenkel-Toledo S, Soroker N. Neurophysiological effects of mirror visual feedback in stroke patients with unilateral hemispheric damage. Brain Res 2018. pii: S0006-8993(18)30458-X.

Beaulieu LD, Milot MH. Changes in transcranial magnetic stimulation outcome measures in response to upper-limb physical training in stroke: a systematic review of randomized controlled trials. Ann Phys Rehabil Med 2018;61(4):224–34.

Beebe JA, Lang CE. Relationships and responsiveness of six upper extremity function tests during the first six months of recovery after stroke. J Neurol Phys Ther 2009;33:96–103.

Bolognini N, Russo C, Edwards DJ. The sensory side of post-stroke motor rehabilitation. Restor Neurol Neurosci 2016;34(4):571–86.

Borich MR, Wolf SL, Tan AQ, Palmer JA. Targeted neuromodulation of abnormal interhemispheric connectivity to promote neural plasticity and recovery of arm function after stroke: a randomized crossover clinical trial study protocol. Neural Plast 2018;2018:9875326.

Boscolo Galazzo I, Storti SF, Formaggio E, Pizzini FB, Fiaschi A, Beltramello A, et al. Investigation of brain hemodynamic changes induced by active and passive movements: a combined arterial spin labeling-BOLD fMRI study. J Magn Reson Imag 2014;40(4):937–48.

Brewer BR, McDowell SK, Worthen-Chaudhari LC. Post-stroke upper extremity rehabilitation: a review of robotic systems and clinical results. Top Stroke Rehabil 2007;14(6):22–44.

Broeks JG, Lankhorst GJ, Rumping K, Prevo AJ. The long-term outcome of arm function after stroke: results of a follow-up study. Disabil Rehabil 1999;21:357–64.

Calabrò RS, Naro A, Russo M, Bramanti P, Carioti L, Balletta T, Buda A, Manuli A, Filoni S, Bramanti A. Shaping neuroplasticity by using powered exoskeletons in patients with stroke: a randomized clinical trial. J Neuroeng Rehabil 2018;15(1):35.

Calabrò RS, Russo M, Naro A, Milardi D, Balletta T, Leo A, Filoni S, Bramanti P. Who may benefit from armeo power treatment? A neurophysiological approach to predict neurorehabilitation outcomes. PM R 2016;8(10):971–8.

Chang WH, Kim YH. Robot-assisted therapy in stroke rehabilitation. J Stroke 2013;15(3):174–81.

Chisari C. Bottom-up or top-down approach? Understanding the way to reach the milestone of recovery in stroke. Int J Neurorehabil 2015;2:e107.

Clarkson AN, Huang BS, Macisaac SE, Mody I, Carmichael ST. Reducing excessive GABA-mediated tonic inhibition promotes functional recovery after stroke. Nature 2010;468(7321):305–9.

Cohen J. Statistical power analysis for the behavioral sciences. 2nd ed. Hillsdale: Lawrence Erlbaum; 1988.

Cooke SF, Bliss TV. Plasticity in the human central nervous system. Brain 2006;129:1659–73.

Croarkin E, Danoff J, Barnes C. Evidence-based rating of upper-extremity motor function tests used for people following a stroke. Phys Ther 2004;84(1):62–74.

da Silva LCP, Paz CCSC, Miranda de Sá AMFL, Tierra-Criollo CJ. EEG coherence analysis in subjects after rehabilitation from stroke with motor imagery. In: Lhotska L, Sukupova L, Lacković I, Ibbott G, editors. World congress on medical physics and biomedical engineering 2018 IFMBE proceedings 2018;vol. 68/2. Singapore: Springer; 2018.

Di Lazzaro V, Profice P, Pilato F, Capone F, Ranieri F, Florio L, Colosimo C, Pravatà E, Pasqualetti P, Dileone M. The level of cortical afferent inhibition in acute stroke correlates with long-term functional recovery in humans. Stroke 2012;43(1):250–2.

Di Lazzaro V, Restuccia D, Oliviero A, Profice P, Ferrara L, Insola A, Mazzone P, Tonali P, Rothwell JC. Magnetic transcranial stimulation at intensities below active motor threshold activates intracortical inhibitory circuits. Exp Brain Res 1998;119:265–8.

Di Pino G, Maravita A, Zollo L, Guglielmelli E, Di Lazzaro V. Augmentation-related brain plasticity. Front Hum Neurosci 2014;8:109.

Engel AK, Fries P. Beta-band oscillations–signalling the status quo? Curr Opin Neurobiol 2010 Apr;20(2):156–65.

Fazekas G, Horvath M, Toth A. A novel robot training system designed to supplement upper limb physiotherapy of patients with spastic hemiparesis. Int J Rehabil Res 2006;3:251–4.

Ferris JK, Neva JL, Francisco BA, Boyd LA. Bilateral motor cortex plasticity in individuals with chronic stroke, induced by paired associative stimulation. Neurorehabil Neural Rep 2018;32(8):671–81.

Formaggio E, Storti SF, Avesani M, Cerini R, Milanese F, Gasparini A, Acler M, Pozzi Mucelli R, Fiaschi A, Manganotti P. EEG and FMRI coregistration to investigate the cortical oscillatory activities during finger movement. Brain Topogr 2008;21(2):100–11.

Formaggio E, Storti SF, Boscolo Galazzo I, Gandolfi M, Geroin C, Smania N, Spezia L, Waldner A, Fiaschi A, Manganotti P. Modulation of event-related desynchronization in robot-assisted hand performance: brain oscillatory changes in active, passive and imagined movements. J Neuroeng Rehabil 2013;10:24.

Formaggio E, Storti SF, Boscolo Galazzo I, Gandolfi M, Geroin C, Smania N, Fiaschi A, Manganotti P. Time-frequency modulation of ERD and EEG coherence in robot-assisted hand performance. Brain Topogr 2015;28(2):352–63.

Fugl-Meyer AR, Jääskö L, Leyman I, Olsson S, Steglind S. The post-stroke hemiplegic patient. 1. A method for evaluation of physical performance. Scand J Rehabil Med 1975;7(1):13–31.

Gladstone DJ, Danells CJ, Black SE. The Fugl-Meyer assessment of motor recovery after stroke: a critical review of its measurement properties. Neurorehab Neural Rep 2002;16(3):232–40.

Hara Y. Brain plasticity and rehabilitation in stroke patients. J Nippon Med Sch 2015;82(1):4–13.

Hatem SM, Saussez G, Della Faille M, Prist V, Zhang X, Dispa D, Bleyenheuft Y. Rehabilitation of motor function after stroke: a multiple systematic review focused on techniques to stimulate upper extremity recovery. Front Hum Neurosci 2016;10:442.

Homan R, Herman J, Purdy P. Cerebral location of international 10/20 system electrode placement. Electroencephalogr Clin Neurophysiol 1987;66:376–82.

Huang X, Naghdy F, Naghdy G, Du H, Todd C. The Combined effects of adaptive control and virtual reality on robot-assisted fine hand motion rehabilitation in chronic stroke patients: a case study. J Stroke Cerebrovasc Dis 2018;27(1):221–8.

Hubbard IJ, Parsons MW, Neilson C, Carey LM. Task-specific training: evidence for and translation to clinical practice. Occup Ther Int 2009;16(3–4):175–89.

Jang SH, Kim YH, Chang Y, Han BS, Byun WM, Chang CH. The predictive value of cortical activation by passive movement for motor recovery in stroke patients. Restor Neurol Neurosci 2004;22(2):59–63.

Johansen-Berg H, Dawes H, Guy C, Smith SM, Wade DT, Matthews PM. Correlation between motor improvements and altered fMRI activity after rehabilitative therapy. Brain 2002;125:2731–42.

Johansson BB. Brain plasticity and stroke rehabilitation. Willis Lect Stroke 2000;31(1):223–30.

Johansson BB. Current trends in stroke rehabilitation. A review with focus on brain plasticity. Acta Neurol Scand 2011;123:147–59.

Kaehlin-Lang A, Luft AR, Sawaki L, Burstein AH, Sohn YH, Cohen LG. Modulation of human corticomotor excitability by somatosensory input. J Physiol 2002;540:623–33.

Kim E, Kovalenko I, Lacey L, Shinohara M, Ueda J. Timing analysis of robotic neuromodulatory rehabilitation system for paired associative stimulation. IEEE Robot Autom Lett 2016;1(2):1028–235.

Krebs HI, Volpe B, Hogan N. A working model of stroke recovery from rehabilitation robotics practitioners. J Neuroeng Rehabil 2009;6:6.

Krebs HI, Volpe BT. Rehabilitation robotics. Handb Clin Neurol 2013;110:283–94.

Kwakkel G, Kolten BJ, Krebs HI. Effects of robot-assisted therapy on upper limb recovery after stroke: a systematic review. Neurorehabil Neural Rep 2008a;22:111–21.

Kwakkel G, Meskers CG, van Wegen EE, Lankhorst GJ, Geurts AC, van Kuijk AA, Lindeman E, Visser-Meily A, de Vlugt E, Arendzen JH. Impact of early applied upper limb stimulation: the EXPLICIT-stroke programme design. BMC Neurol 2008b;8:49.

Lai SM, Studenski S, Duncan PW, Perera S. Persisting consequences of stroke measured by the Stroke Impact Scale. Stroke 2002;33:1840–4.

Lam TK, Dawson DR, Honjo K, Ross B, Binns MA, Stuss DT, Black SE, Chen JJ, Levine BT, Fujioka T, Chen JL. Neural coupling between contralesional motor and frontoparietal networks correlates with motor ability in individuals with chronic stroke. J Neurol Sci 2018;384:21–9.

Leocani L, Toro C, Manganotti P, Zhuang P, Hallett M. Event-related coherence and event-related desynchronization/synchronization in the 10 Hz and 20 Hz EEG during self-paced movements. Electroencephalogr Clin Neurophysiol 1997;104:199–206.

Liu H, Song LP, Zhang T. Mental practice combined with physical practice to enhance hand recovery in stroke patients. Behav Neurol 2014;2014:876416.

Lo AC. Clinical designs of recent robot rehabilitation trials. Am J Phys Med Rehabil 2012;91:S204–16.

Loubinoux I, Carel C, Pariente J, Dechaumont S, Albucher JF, Marque P, et al. Correlation between cerebral reorganization and motor recovery after subcortical infarcts. Neuroimage 2003;20:2166–80.

Lum PS, Godfrey SB, Brokaw EB, Holley RJ, Nichols D. Robotic approaches for rehabilitation of hand function after stroke. Am J Phys Med Rehabil 2012;91(11S3):S242–54.

Maciejasz P, Eschweiler J, Gerlach-Hahn K, Jansen-Troy A, Leonhardt S. A survey on robotic devices for upper limb rehabilitation. J Neuroeng Rehabil 2014;11:3.

Manganotti P, Gerloff C, Toro C, Katsuta H, Sadato N, Zhuang Leocani L, Hallett M. Task-related coherence and task-related spectral power changes during sequential finger movements. Electroencephalogr Clin Neurophysiol 1998;109(1):50–62.

Matteis M, Vernieri F, Troisi E, Pasqualetti P, Tibuzzi F, Caltagirone C, Silvestrini M. Early cerebral hemodynamic changes during passive movements and motor recovery after stroke. J Neurol 2003;250(7):810–7.

Mehrholz J, Hädrich A, Platz T, Kugler J, Pohl M. Electromechanical and robot-assisted arm training for improving generic activities of daily living, arm function, and arm muscle strength after stroke. Cochrane Database Syst Rev 2012;6:CD006876.

Mehrholz J, Platz T, Kugler J, Pohl M. Electromechanical and robot-assisted arm training for improving arm function and activities of daily living after stroke. Cochrane Database Syst Rev 2008;4:CD006876.

Mihara M, Hattori N, Hatakenaka M, Yagura H, Kawano T, Hino T, et al. Near-infrared spectroscopy-mediated neurofeedback enhances efficacy of motor imagery-based training in post-stroke victims: a pilot study. Stroke 2013;44:1091–8.

Müller-Putz GR, Zimmermann D, Graimann B, Nestinger K, Korisek G, Pfurtscheller G. Event-related beta EEG-changes during passive and attempted foot movements in paraplegic patients. Brain Res 2007;1137(1):84–91.
Nakayashiki K, Saeki M, Takata Y, Hayashi Y, Kondo T. Modulation of event-related desynchronization during kinematic and kinetic hand movements. J Neuroeng Rehabil 2014;11:90.
Nardone R, Tezzon F. Inhibitory and excitatory circuits of cerebral cortex after ischaemic stroke: prognostic value of the transcranial magnetic stimulation. Electromyogr Clin Neurophysiol 2002;42(3):131–6.
Neuper C, Scherer R, Reiner M. Pfurtscheller G Imagery of motor actions: differential effects of kinesthetic and visual-motor mode of imagery in single-trial EEG. Brain Res Cogn Brain Res 2005;25(3):668–77.
Nie J, Yang X. Modulation of synaptic plasticity by exercise training as a basis for ischemic stroke rehabilitation. Cell Mol Neurobiol 2017;37(1):5–16.
Nirkko AC, Ozdoba C, Redmond SM, Bürki M, Schroth G, Hess CW, Wiesendanger M. Different ipsilateral representations for distal and proximal movements in the sensorimotor cortex: activation and deactivation patterns. Neuroimage 2001;13 (5):825–35.
Noppeney U, Price CJ, Penny WD, Friston KJ. Two distinct neural mechanisms for category-selective responses. Cereb Cortex 2006;16:437–45.
Norouzi-Gheidari N, Archambault PS, Fung J. Effects of robot-assisted therapy on stroke rehabilitation in upper limbs: systematic review and meta-analysis of the literature. J Rehabil Res Dev 2012;49(4):479–96.
Novakovic V, Sanguineti V. Adaptation to constant-magnitude assistive forces: kinematic and neural correlates. Exp Brain Res 2011;209:425–36.
Nudo RJ. Recovery after brain injury: mechanisms and principles. Front Hum Neurosci 2013;7:887.
Palmer JA, Wolf SL, Borich MR. Paired associative stimulation modulates corticomotor excitability in chronic stroke: a preliminary investigation. Restor Neurol Neurosci 2018;36(2):183–94.
Paulus W, Classen J, Cohen LG, Large CH, Di Lazzaro V, Nitsche M, Ziemann U. State of the art: pharmacologic effects on cortical excitability measures tested by transcranial magnetic stimulation. Brain Stimul 2008;1(3):151–63.
Pekna M, Pekny M, Nilsson M. Modulation of neural plasticity as a basis for stroke rehabilitation. Stroke 2012;43(10):2819–28.
Pfurtscheller G, Aranibar A. Event-related cortical desynchronization detected by power measurements of scalp EEG. Electroencephalogr Clin Neurophysiol 1977;42(6):817–26.
Pollock A, Farmer SE, Brady MC, Langhorne P, Mead GE, Mehrholz J, van Wijck F. Interventions for improving upper limb function after stroke. Cochrane Database Syst Rev 2014(11):CD010820.
Pool EM, Leimbach M, Binder E, Nettekoven C, Eickhoff SB, Fink GR, Grefkes C. Network dynamics engaged in the modulation of motor behavior in stroke patients. Hum Brain Mapp 2018;39(3):1078–92.
Prieto GA, Cano-de-la-Cuerda R, López-Larraz E, Metrot J, Molinari M, van Dokkum LHE. Emerging perspectives in stroke rehabilitation. In Pons JL, Torricelli D, editors, Emerging therapies in neurorehabilitation. BioSysRob, vol. 4; 2014. p. 3–21.
Quartarone A, Rizzo V, Bagnato S, Morgante F, Sant'Angelo A, Girlanda P, Siebner HR. Rapid-rate paired associative stimulation of the median nerve and motor cortex can produce long-lasting changes in motor cortical excitability in humans. J Physiol 2006;575(2):657–70.
Ramos-Murguialday A, Birbaumer N. Brain oscillatory signatures of motor tasks. J Neurophysiol 2015;113(10):3663–82.
Ramos-Murguialday A, Schurholz M, Caggiano V, Wilbruger M, Caria A, Hammer EM, et al. Proprioceptive feedback and brain computer interface (BCI) based neuroprostheses. PLoS One 2012;7:e47048.
Roby-Brami A, Feydy A, Combeaud M, Biryukova EV, Bussel B, Levin MF. Motor compensation and recovery for reaching in stroke patients. Acta Neurol Scand 2003;107(5):369–81.
Rosenthal JA. Qualitative descriptors of strength of association and effect size. J Social Serv Res 1996;21(4):37–59.
Sale P, Lombardi V, Franceschini M. Hand robotics rehabilitation: feasibility and preliminary results of a robotic treatment in patients with hemiparesis. Stroke Res Treat 2012;2012:820931.
Sale P, Mazzoleni S, Lombardi V, Galafate D, Massimiani MP, Posteraro F, Damiani C, Franceschini M. Recovery of hand function with robot-assisted therapy in acute stroke patients: a randomized-controlled trial. Int J Rehabil Res 2014;37 (3):236–42.
Santisteban L, Térémetz M, Bleton JP, Baron JC, Maier MA, Lindberg PG. Upper Limb outcome measures used in stroke rehabilitation studies: a systematic literature review. PLoS One 2016;11(5):e0154792.
Semprini M, Cuppone AV, Delis I, Squeri V, Panzeri S, Konczak J. Biofeedback signals for robotic rehabilitation: assessment of wrist muscle activation patterns in healthy humans. IEEE Trans Neural Syst Rehabil Eng 2017;25(7):883–92.
Seo HY, Kim G-W, Won YH, Park S-H, Seo J-H, Ko M-H. Changes in intracortical excitability of affected and unaffected hemispheres after stroke evaluated by paired-pulse transcranial magnetic stimulation. Ann Rehabil Med 2018;42 (4):495–501.
Sergi F, Krebs HI, Groissier B, Rykman A, Guglielmelli E, Volpe BT, et al. Predicting efficacy of robot-aided rehabilitation in chronic stroke patients using an MRI-compatible robotic device. In: Conf Proc IEEE Eng Med Biol Soc (2011). p. 7470–3.
Simonetta-Moreau M. Non-invasive brain stimulation (NIBS) and motor recovery after stroke. Ann Phys Rehabil Med 2014;57(8):530–42.
Sivan M, O'Connor RJ, Makower S, Levesley M, Bhakta B. Systematic review of outcome measures used in the evaluation of robot-assisted upper limb exercise in stroke. J Rehabil Med 2011;43(3):181–9.
Spalletti C, Alia C, Lai S, Panarese A, Conti S, Micera S, Caleo M. Combining robotic training and inactivation of the healthy hemisphere restores pre-stroke motor patterns in mice. eLife 2017;6:e28662.
Stein J, Bishop L, Gillen G, Helbok R. Robot-assisted exercise for hand weakness after stroke: a pilot study. Am J Phys Med Rehabil 2011;90(11):887–94.
Stippich C, Ochmann H, Sartor K. Somatotopic mapping of the human primary sensorimotor cortex during motor imagery and motor execution by functional magnetic resonance imaging. Neurosci Lett 2002;331(1):50–4.
Takano B, Drzezga A, Peller M, Sax I, Schwaiger M, Lee L, Siebner HR. Short-term modulation of regional excitability and blood flow in human motor cortex following rapid-rate transcranial magnetic stimulation. Neuroimage 2004;23:849–59.
Takeuchi N, Izumi S. Combinations of stroke neurorehabilitation to facilitate motor recovery: perspectives on Hebbian plasticity and homeostatic metaplasticity. Front Hum Neurosci 2015;9:349.
Takeuchi N, Izumi S. Maladaptive plasticity for motor recovery after stroke: mechanisms and approaches. Neural Plast 2012b;2012:359728.
Takeuchi N, Izumi S. Rehabilitation with poststroke motor recovery: a review with a focus on neural plasticity. Stroke Res Treat 2013;2013:128641.
Takeuchi N, Oouchida Y, Izumi S-I. Motor control and neural plasticity through interhemispheric interactions. Neural Plast 2012a;2012:823285.
Tokimura H, Di Lazzaro V, Tokimura Y, Oliviero A, Profice P, Insola A, Mazzone P, Tonali P, Rothwell JC. Short latency inhibition of human hand motor cortex by somatosensory input from the hand. J Physiol 2000;523(2):503–13.
Tolmacheva A, Savolainen S, Kirveskari E, Lioumis P, Kuusela L, Brandstack N, et al. Long-term paired associative stimulation enhances motor output of the tetraplegic hand. J Neurotrauma 2017;34(18):2668–74.
Turco CV, Locke MB, El-Sayes J, Tommerdahl M, Nelson AJ. Exploring behavioral correlates of afferent inhibition. Brain Sci 2018;8(4):64.
Turner DL, Ramos-Murguialday A, Birbaumer N, Hoffmann U, Luft A. Neurophysiology of robot-mediated training and therapy: a perspective for future use in clinical populations. Front Neurol 2013;4:18.
Ward N, Brown M, Thompson A, Frackowiak R. Neural correlates of outcome after stroke: a cross-sectional fMRI study. Brain 2003;126:1430–48.
Weder BJ, Wiest R, Seitz RJ. Principles underlying post-stroke recovery of upper extremity sensorimotor function – a neuroimaging perspective. SA: Frontiers Media; 2016.
Wei W, Bai L, Wang J, Dai R, Tong RK, Zhang Y, et al. A longitudinal study of hand motor recovery after sub-acute stroke: a study combined FMRI with diffusion tensor imaging. PLoS One 2013;8:e64154.
Wolters A, Sandbrink F, Schlottmann A, Kunesch E, Stefan K, Cohen LG, Benecke R, Classen J. A temporally asymmetric Hebbian rule governing plasticity in the human motor cortex. J Neurophysiol 2003;89:2339–45.
Woytowicz EJ, Rietschel JC, Goodman RN, Conroy SS, Sorkin JD, Whitall J, McCombe Waller S. Determining levels of upper extremity movement impairment by applying a cluster analysis to the Fugl-Meyer assessment of the upper extremity in chronic stroke. Arch Phys Med Rehabil 2016;98(3):456–62.
Wu J, Quinlan EB, Dodakian L, McKenzie A, Kathuria N, Zhou RJ, Augsburger R, See J, Le VH, Srinivasan R, Cramer SC. Connectivity measures are robust biomarkers of cortical function and plasticity after stroke. Brain 2015;138(Pt 8):2359–69.
Yue Z, Zhang X, Wang J. Hand rehabilitation robotics on poststroke motor recovery. Behav Neurol 2017;2017:3908135.
Zhao Z, Wu J, Fan M, Yin D, Tang C, Gong J, Xu G, Gao X, Yu Q, Yang H, Sun L, Jia J. Altered intra- and inter-network functional coupling of resting-state networks associated with motor dysfunction in stroke. Hum Brain Mapp 2018;39 (8):3388–97.
Zou Y, Zhao Z, Yin D, Fan M, Small M, Liu Z, Hilgetag CC, Kurths J. Brain anomaly networks uncover heterogeneous functional reorganization patterns after stroke. Neuroimage Clin 2018;20:523–30.